Growth of CoCrTa$(11\bar{2}0)$-oriented thin films on a D0$_3$ Mn$_3$Si(002) underlayer

Yu-Nu Hsu,[a] David E. Laughlin, and David N. Lambeth
Data Storage System Center, Carnegie Mellon University, Pittsburgh, Pennsylvania 15213

Mn_3Si possesses a D0$_3$ structure, which is a bcc derivative structure with nearly the same atomic spacing as Cr and NiAl which have been commonly used for longitudinal magnetic recording underlayers. AG(30 nm)/CoCrTa(40 nm)/Mn_3Si(x, $x=100$, 200, 400 nm)/Ag(75 nm) thin films were sputter deposited onto hydrofluoric acid (HF)-etched Si:(001) substrates at elevated temperature. Compared to the 100 and 200 nm thick Mn_3Si samples, the XRD spectrum of the 400 nm thick Mn_3Si sample shows a significant increase in the intensity of the Mn_3Si(002) peak. This suggests that a high volume fraction of the D0$_3$ phase was formed. The CoCrTa$(11\bar{2}0)$ peak intensity has been found to increase with Mn_3Si thickness. As a result, the in-plane coercivity increases as the volume fraction of the D0$_3$ phase increases. [S0021-8979(00)88408-X]

For high density longitudinal magnetic recording, it is essential to align the Co *c* axis in the thin film plane. There are two ways of achieving this, both are based on close atomic matching of a magnetic layer with an underlayer. One is to epitaxially grow bicrystal Co$(11\bar{2}0)$/Cr(002)[1] and the other is to epitaxially grow unicrystal Co$(10\bar{1}0)$/Cr(112)/NiAl(112)[2] texture films. For the Co bicrystal $(11\bar{2}0)$-textured magnetic layer, there are two crystallographically orthogonal variants whose *c* axes can lie perpendicular to each other on a single Cr grain.

The new D0$_3$ Mn_3Si underlayer has a lattice parameter of 5.72 Å, which is twice as large as that of the Cr and NiAl underlayers. The D0$_3$ structure is a bcc derivative structure. If one imagines all of the atoms are the same, the unit cell consists of eight bcc unit cells. The D0$_3$ structure has an fcc Bravais lattice with Si atoms sitting at the fcc lattice sites and Mn atoms occupying all of the octahedral and tetrahedral sites of the lattice.[3] The single-phase Mn_3Si is stable only between 25 and 25.6 at % of Si and then only above 677 °C.[4] In this study, a Ag(001)/Si(001) template was used to stabilize the D0$_3$ Mn_3Si phase at lower temperature and epitaxially induce the Mn_3Si(002)-textured thin film. The epitaxial growth of CoCrTa$(11\bar{2}0)$-textured thin film is also found to be induced by the D0$_3$ Mn_3Si(002)-textured underlayer.

Ag(001)/Si(001) templates have been shown by Yang *et al.* to epitaxially induce the bicrystal Co$(11\bar{2}0)$ thin films when grown on a Cr(002) epitaxially grown underlayer.[5] The misfit between the fcc Ag ($a=4.09$ Å) and diamond cubic Si ($a=5.43$ Å) is 24.7% (very close to $\frac{1}{4}$). It has been shown by Yang *et al.* that a 4×4 mesh of Ag unit cells fits very well onto a 3×3 mesh of Si unit cell with a mismatch of only 0.4%.[5] Likewise, due to the small lattice mismatch (~0.2%) between the atomic spacings of the Ag(001) and Mn_3Si(002) planes, the Mn_3Si(002)-textured film was found to grow epitaxially onto the Ag(001) films. Because the atomic spacing of the Mn_3Si\{110\} planes ($d=4.07$ Å) is about the same as that of the Ag \{100\} planes ($d=4.09$ Å), the Mn_3Si(002) plane rotates 45° to fit the Ag(001) plane as shown in Fig. 1(a). As a result, it leads the epitaxial relationship of Ag and Mn_3Si to be Ag(001)[100]‖Mn_3Si(002)[110]. In addition, the lattice mismatch calculated from the atomic spacing between CoCrTa and Mn_3Si is 7.8% perpendicular to the Co *c* axis and 2.0% along the Co *c* axis. The schematic in Fig. 1(b) shows the epitaxial relationship between Co$(11\bar{2}0)$ and Mn_3Si(002) planes. The Mn_3Si(002) plane can match with the Co$(11\bar{2}0)$ plane with the Co *c* axis aligned along either the Mn_3Si[110] or $[1\bar{1}0]$ direction.

The Ag/CoCrTa/Mn_3Si/Ag thin films were deposited on single-crystal Si(100) substrates by rf diode sputtering in an Leybold–Heraeus Z-400 system. To remove the oxide layers, the Si(100) substrates were hydrofluoric acid (HF)-etched.[5] The base pressure was 7×10^{-7} mTorr. The $Co_{84}Cr_{13}Ta_3$ and overcoat Ag films were deposited at 150 °C (measured by a temperature label) with a fixed argon pres-

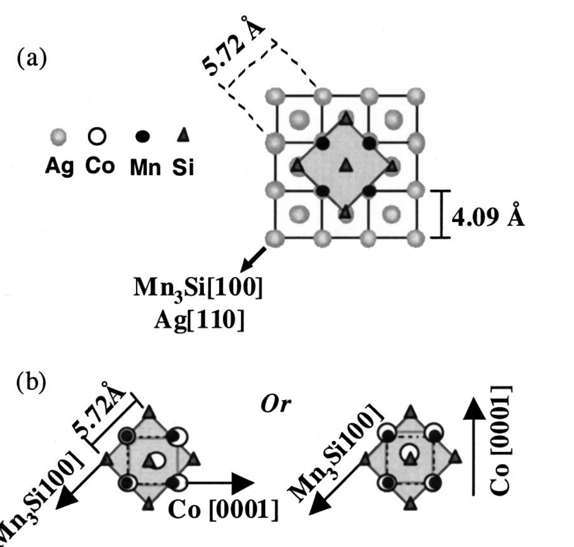

FIG. 1. Schematic of the epitaxial relationships of (a) Ag(001)[110]‖Mn_3Si(002)[100] and (b) Mn_3Si(002)[110]‖CoCrPt$(11\bar{2}0)$[0001].

[a]Electronic mail: yh2a@andrew.cmu.edu

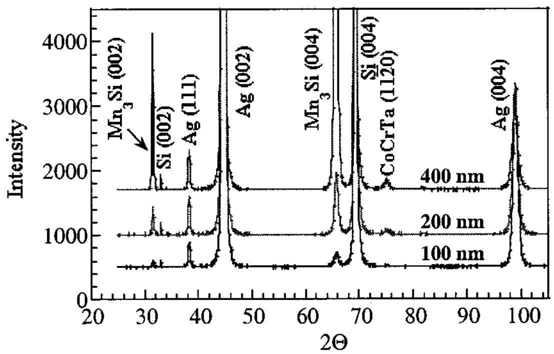

FIG. 2. X-ray $\theta/2\theta$ diffraction spectra of the Ag(30 nm)/CoCrTa(40 nm)/Mn_3Si(x,$x=100$, 200, 400 nm)/Ag(75 nm) thin films.

sure of 10 mTorr, rf power of 2.3 W/cm^2 and without substrate bias voltage. The Mn_3Si and Ag underlayers were deposited at 10 mTorr, zero substrate bias, 300 °C (measured by the temperature label), and at the sputtering powers of 6.9 and 2.3 W/cm^2, respectively. The thickness of the Ag overcoat, CoCrTa, and Ag underlayer films were fixed at 30, 40, and 75 nm, respectively. The thickness of the Mn_3Si films was varied. The epitaxial orientation relationship was studied by both $\theta/2\theta$ and ϕ scans on a Rigaku x-ray diffractometer with Cu $K\alpha$ radiation as well as with a Philips EM 420T transmission electron microscope (TEM). Magnetic properties of the thin films were measured using a vibrating sample magnetometer (VSM) with fields up to 10 kOe.

Figure 2 shows the x-ray $\theta/2\theta$ diffraction spectra for the Ag(30 nm)/CoCrTa(40 nm)/Mn_3Si(x,$x=100$, 200, 400 nm)/Ag(75 nm)/Si(001) samples. Strong Ag(002) and (004) peaks appear in all of these spectra, indicating very strong Ag(002) texture in the Ag/Si template. As the Mn_3Si thickness increases, the x-ray diffraction intensity of the Mn_3Si(002) and (004) peaks enhances more significantly than linearly with film thickness. This shows that the Mn_3Si underlayers become more (002) oriented as the Mn_3Si underlayer thickness increases. It is noticed that the CoCrTa($11\bar{2}0$) x-ray diffraction peaks are also enhanced with the increasing Mn_3Si underlayer thickness, which implies the improvement of the Mn_3Si texture. The Ag (111) peak results from the Ag overcoat and not from the underlayer.

The ϕ scan spectra of the Mn_3Si(400 nm)/Ag(75 nm)/Si(100) are shown in Fig. 3. As expected from the cubic crystal (001) stereographic projection, four diffraction peaks, 90° apart, were found in the Si, Ag, and Mn_3Si\{220\} pole ϕ scan spectra. The positions of the four \{220\} poles for the single-crystal Si(001) substrate and Ag are the same, confirming the epitaxial cube on cube relationship between the Si[220] and Ag[220] directions. The positions of the four Mn_3Si\{220\} poles shift 45° when compared to those of the Ag and Si\{220\} poles, which indicates that the Mn_3Si[220] direction is parallel to the Ag and Si[100] direction and in agreement with the epitaxial orientations shown in Fig. 1(a).

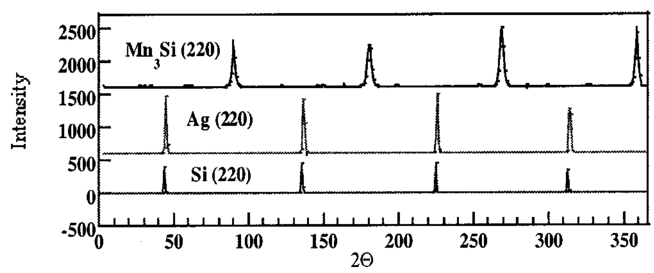

FIG. 3. Si \{220\}pole, Ag\{220\} pole, and Mn_3Si\{220\} pole x-ray ϕ scan diffraction spectra of the Mn_3Si(400 nm)/Ag(75 nm) thin films.

TEM was also used to investigate the epitaxial relationship of the thin film. Figures 4(a) and 4(b) show the TEM selected area diffraction and simulated pattern of the Mn_3Si(400 nm)/Ag(75 nm) thin films, respectively. They show the Ag(001) zone axis to be parallel to the Mn_3Si(002) zone axis. The overlap of the Ag\{200\} and Mn_3Si\{220\} diffraction spots indicates a close atomic spacing between Ag\{200\} and Mn_3Si\{220\} planes. This also shows that the Ag(001) planes rotate 45° to fit the Mn_3Si(001) planes. The epitaxial relationship of the Ag(001)[100]$\|$$Mn_3Si$(002)[110] is evident from this diffraction pattern.

Figures 4(c) and 4(d) show the TEM selected area diffraction and simulated pattern of the CoCrTa(40 nm)/Mn_3Si(400 nm)/Ag(75 nm) thin films, respectively. Because the bicrystal CoCrTa($11\bar{2}0$) plane fits the Mn_3Si(002) plane in two ways with the c axes perpendicular to each other, there are two sets of CoCrTa($11\bar{2}0$) zone axis diffraction patterns perpendicular to each other in Figs. 4(c) and 4(d). Both of the CoCrTa TEM diffraction patterns from the ($11\bar{2}0$) zone axis have the Co\{0002\} reflections overlapping with the Mn_3Si\{220\} and Ag\{200\} reflections. This indicates that the epitaxial relationship of the CoCrTa/Mn_3Si/Ag thin film are CoCrTa($11\bar{2}0$)[0002]$\|$$Mn_3Si$(002)[110]$\|$Ag(001)[100]. Combined with the epitaxial relationship of the Ag(100)/Si(100) template investigated by Yang *et al.* as Ag(100)[100]$\|$Si(100)[100],[5] the overall epitaxial relationship can be determined as CoCrTa($11\bar{2}0$)[0002]$\|$$Mn_3Si$(002)[110]$\|$Ag(001)[100]$\|$Si(001)[100]. Ring patterns are also seen in these TEM diffraction patterns, indicating that while most of the grains grow epitaxially, a portion of them grow with random orientations relative to the Si substrate.

The magnetic properties of the Ag(30 nm)/CoCrTa(40 nm)/Mn_3Si/Ag(75 nm)/Si(100) thin films were found to vary with the Mn_3Si underlayer thickness, as shown in Fig. 5. The coercivity of the Ag(30 nm)/CoCrTa(40 nm)/Mn_3Si/Ag(75 nm)/Si(100) thin films increases from 347, 737 to 848 Oe at the Mn_3Si thickness of 100, 200, and 400 nm, respectively. This is thought to be due to the enhanced CoCrTa($11\bar{2}0$) texture as the Mn_3Si(200) texture improves with the Mn_3Si thickness. Conceptually, the reduced coercivity could be caused by the Co grains with random orientation.

In this study, the $D0_3$-structured Mn_3Si phase has been stabilized via the employment of the Ag(001)/Si(001) template. Mn_3Si(002) texture has been shown to be induced by the Ag(001)/Si(001) template, which in turn induced the epitaxial growth of the CoCrTa($11\bar{2}0$) bicrystal. The orientation relationship of the CoCrTa/Mn_3Si/Ag/Si(001) structure was determined by the x-ray $\theta/2\theta$ and ϕ scan diffraction

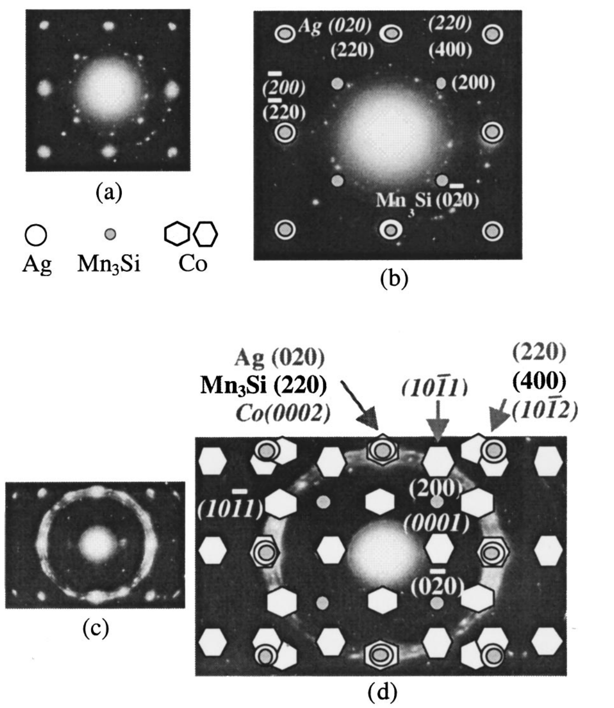

FIG. 4. (a) TEM selected area diffraction and (b) simulated pattern of the of the zone axes of the Ag[001] and Mn_3Si[001] of the CoCrTa(40 nm)/Mn_3Si(400 nm)/Ag(75 nm) thin films. (c) TEM selected area diffraction and (d) simulated pattern of the zone axes of the CoCrPt[$11\bar{2}0$], Ag[001] and Mn_3Si[001] of the CoCrTa(40 nm)/Mn_3Si(400 nm)/Ag(75 nm) thin films.

methods as well as TEM. As the Mn_3Si thickness increases, the Mn_3Si(002) texture was shown to be enhanced significantly, which in turn enhanced the CoCrTa($11\bar{2}0$) texture and increased the CoCrTa in-plane coercivity.

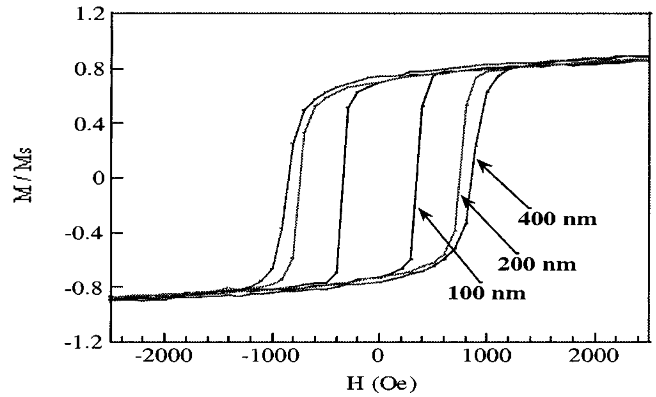

FIG. 5. In-plane hysteresis loops of the Ag(30 nm)/CoCrTa(40 nm)/Mn_3Si(x, x = 100, 200, 400 nm)/Ag(75 nm) thin films deposited onto the single-crystal Si(001) substrates.

The authors gratefully thank Dr. Lu Bin and Mr. Sangki Jeong for valuable discussions. This research is supported by the Data Storage Systems Center at CMU under a Grant No. ECD-89-07068 from National Science Foundation. The government has certain rights to this material.

[1] Y.-P. Deng, D. N. Lambeth, L.-L. Lee, and D. E. Laughlin, J. Appl. Phys. **73**, 6677 (1993).
[2] L.-L. Lee, D. E. Laughlin, and D. N. Lambeth, IEEE Trans. Magn. **30**, 3951 (1994).
[3] P. Villars and L. D. Calvert, *Pearson's Handbook of Crystallographic Data for Intermetallic Phases* (ASM International, Metals Park, OH, 1991).
[4] T. B. Massalski, *Binary Alloy Phase Diagrams* (ASM International, Metals Park, OH, 1996).
[5] W. Yang, D. N. Lambeth, L. Tang, and D. E. Laughlin, J. Appl. Phys. **81**, 4370 (1997).